Received: 8 October 2019 | Revised: 18 January 2020 | Accepted: 28 January 2020

DOI: 10.1111/cmi.13181

RESEARCH ARTICLE

WILEY

Hepatitis B subviral envelope particles use the COPII machinery for intracellular transport via selective exploitation of Sec24A and Sec23B

Lisa Zeyen[1] | Tatjana Döring[1] | Jens T. Stieler[2] | Reinhild Prange[1]

[1]Department of Virology, University Medical Center of the Johannes Gutenberg University Mainz, Mainz, Germany

[2]Department of Molecular and Cellular Mechanisms of Neurodegeneration, Paul Flechsig Institute of Brain Research, University of Leipzig, Leipzig, Germany

Correspondence
Reinhild Prange, Department of Virology, University Medical Center of the Johannes Gutenberg University Mainz, Augustusplatz, D-55131 Mainz, Germany.
Email: prange@uni-mainz.de

Funding information
Deutsche Forschungsgemeinschaft, Grant/Award Number: PR 305/3-2/3-3

Abstract

Hepatitis B virus (HBV) is a leading cause of liver disease. Its success as a human pathogen is related to the immense production of subviral envelope particles (SVPs) contributing to viral persistence by interfering with immune functions. To explore cellular pathways involved in SVP formation and egress, we investigated host–pathogen interactions. Yeast-based proteomics revealed Sec24A, a component of the coat protein complex II (COPII), as an interaction partner of the HBV envelope S domain. To understand how HBV co-opts COPII as a proviral machinery, we studied roles of key Sec proteins in HBV-expressing liver cells. Silencing of Sar1, Sec23, and Sec24, which promote COPII assembly concomitant with cargo loading, strongly diminished endoplasmic reticulum (ER) envelope export and SVP secretion. By analysing Sec paralog specificities, we unexpectedly found that the HBV envelope is a selective interaction partner of Sec24A and Sec23B whose functions could not be substituted by their related isoforms. In support, we found that HBV replication upregulated Sec24A and Sec23B transcription. Furthermore, HBV encountered the Sec24A/Sec23B complex via an interaction that involved the N-terminal half of Sec24A and a di-arginine motif of its S domain, mirroring a novel ER export code. Accordingly, an interference with the COPII/HBV cross-talk might display a tool to effectively inhibit SVP release.

KEYWORDS
diseases, infection, microbe–cell interaction, proteomics, viruses

1 | INTRODUCTION

About 1 million deaths per year and more than 250 million chronic infections characterize the hepatitis B virus (HBV) as one of the most successful pathogens and global threat to human health. This is especially remarkable as HBV, an enveloped DNA virus, contains a genome of only about 3 kb in size—one of the smallest viral genomes known (Hu & Seeger, 2015; Nassal, 2008). Despite intense research on HBV since its discovery in the 1960s, there are still no therapeutics available to cure chronic infections that frequently lead to liver cirrhosis and hepatocellular carcinoma (Revill et al., 2019). Its limited genome size forces the virus to interact closely with the host's cellular pathways and to recruit numerous proteins in order to complete its life cycle (Prange, 2012). Therefore, wide investigations of virus–host interactions have become more and more valuable for future perspectives of effective antiviral treatments.

HBV infects hepatocytes of humans and some non-human primates, entering the cell via the bile acid transporter sodium taurocholate cotransporting polypeptide (W. Li, 2015). Its pathogenic life cycle involves a replication by protein-primed reverse transcription and the expression of viral proteins encoded by four open reading frames (ORFs): the polymerase; the capsid-forming core protein and its related preCore derivative; three versions of the envelope proteins termed small (S), middle (M), and large (L); and the transcription regulatory protein X (Blondot, Bruss, & Kann, 2016; Hu & Seeger, 2015; Nassal, 2008). Upon infection of the liver cell, the viral nucleocapsid (NC) gets released out of the envelope and is transported into the nucleus. There, the partially double-stranded viral genome is converted into a covalently closed circular DNA, which then serves as a template for RNA transcription and translation into the viral proteins in the cytoplasm (Blondot et al., 2016; Hu & Seeger, 2015; Nassal, 2008). The DNA-containing NCs become enveloped by the viral S, M, and L proteins that originate from the endoplasmic reticulum (ER) membrane, and the infectious HBV particles finally exit the cell, involving functions of the cellular endosomal sorting complexes required for transport machinery (Chou, Tsai, Huang, Chang, & Shih, 2015; Jiang, Himmelsbach, Ren, Boller, & Hildt, 2015; Stieler & Prange, 2014; Watanabe et al., 2007).

One distinct feature of HBV's life cycle is the production and release of various incomplete and non-infectious particles in addition to the mature virions. Besides genome-free virions, RNA-containing virions, naked NCs, and empty subviral envelope particles (SVPs) are produced consisting of only the viral envelope proteins (Hu & Liu, 2017; Prange, 2012). Remarkably, SVP types, also referred to as hepatitis B surface antigen (HBsAg) particles, are secreted in extreme surplus compared with the infectious HBV particles and are thought to act as decoys to the immune system, thereby exhausting B and T cell responses and contributing to viral persistence (Hu & Liu, 2017; Mohebbi, Lorestani, Tahamtan, Kargar, & Tabarraei, 2018). Confronting the host with several distinct particle types in huge amounts might also be one of the reasons for HBV's immense success as a human pathogen.

One of the most remarkable evolutionary features of eukaryotic cells is the advanced intracellular organization into several membrane-bound compartments or organelles (Rout & Field, 2017). For communication between those compartments, selective vesicular and non-vesicular transport mechanisms for lipids and proteins have developed (Kirchhausen, 2000). Therefore, membrane-manipulating machines acting in exocytosis, endocytosis, and intracellular vesicular transport have emerged to be the key players in eukaryotic cellular organization (Rout & Field, 2017). Discovered in the 1990s, the coat protein complex II (COPII) has been identified as a vesicular transport machinery, moving secretory cargos from the ER to the Golgi apparatus. The anterograde ER-to-Golgi transport is promoted by COPII-coated vesicles via two coexisting mechanisms. The first one is passive, termed bulk flow, in which any ER-localized cargo can be non-selectively encapsulated into COPII vesicles. The second, more efficient mechanism is an active sorting of cargo proteins based on specific signals. Upon ER export, specific Sec proteins function in a highly conserved signal pathway in order to form COPII-coated vesicles, budding out of the ER membrane at ER exit sites (ERESs; Barlowe & Helenius, 2016; Bethune & Wieland, 2018; McCaughey & Stephens, 2018; Miller & Schekman, 2013). COPII assembly starts with the activation of the small GTPase Sar1 and its recruitment to the ER with assistance of its membrane-bound guanine nucleotide exchange factor Sec12. GTP-loading thereby results in a conformational change of Sar1, as its amino-terminal amphipathic helix penetrates the ER membrane to form a curvature—a first step towards vesicle formation. Upon activation, Sar1 recruits the Sec23/Sec24 dimer to build the inner coat layer. Sec24 hereby specifically binds to cargo proteins via distinct binding motifs, whereas Sec23 modulates the GTP cycle of Sar1. After this, the tetrameric Sec13/Sec31 complex gets recruited to the Sar1–Sec23/24 complex in order to form the outer coat layer, sustain the membrane curvature, inactivate Sar1, and finally promote the vesicle budding (Figure 1; Barlowe & Helenius, 2016; Bethune & Wieland, 2018; McCaughey & Stephens, 2018; Miller & Schekman, 2013).

Pathogens like the hepatitis C virus (HCV) and Ebola virus have been shown to utilize COPII as a transport mechanism for viral proteins en route to viral assembly and budding sites (Syed, Khan, Yang, & Siddiqui, 2017; Yamayoshi et al., 2008). Hence, the COPII machinery can become a distinct ally regarding pathogenic morphogenesis and release. Previous proteomics of pathogen–host interactions revealed the inner coat protein Sec24A as a direct binding partner of HBV envelope proteins (Awe, 2009). Trying to unravel possible functions of the COPII machinery or scattered Sec proteins in HBV pathogenesis, we here investigated the impact of interferences with this transport mechanism on subviral maturation and egress.

2 | METHODS

2.1 | Plasmids

The expression vector carrying the HBV S envelope gene, derived from genotype D (GenBank™ accession number V01460), with a C-terminal fused influenza virus hemagglutinin (HA) epitope tag (S.HA) under the transcriptional control of the human metallothionein (hMT) IIA had been described (pNI2.S.HA; Hartmann-Stuhler & Prange, 2001). The mutant S genes were created by mutagenesis using the Q5® Site-Directed Mutagenesis Kit (New England Biolabs). Plasmid p123, carrying the HBV S gene under the control of its natural promoter, was generously provided by C. Sureau (Paris) and was equipped with a C-terminal HA-tag. The plasmid pNI2.L_OHA encodes the HBV L envelope gene within the so-called L_O-(only)-background in which synthesis of the S and M proteins is prevented by missense mutations of their initiator codons. The mutant L_OR78A.HA and L_OR79A.HA constructs had been described previously (Lambert, Mann, & Prange, 2004). To create the HBV preC expression vector, the S gene present in pNI2.S.HA was replaced by the preC ORF. For HBV replication, the episomal expression vector pCEP4ΔCMVΔSV40/1.1xHBV (pHBV), carrying a 1.1× unit length HBV genome, was used (Stieler & Prange, 2014). Plasmid constructs used in the yeast two-hybrid (Y2H) assay screens had been described previously (Awe, 2009). A cDNA clone encoding the short

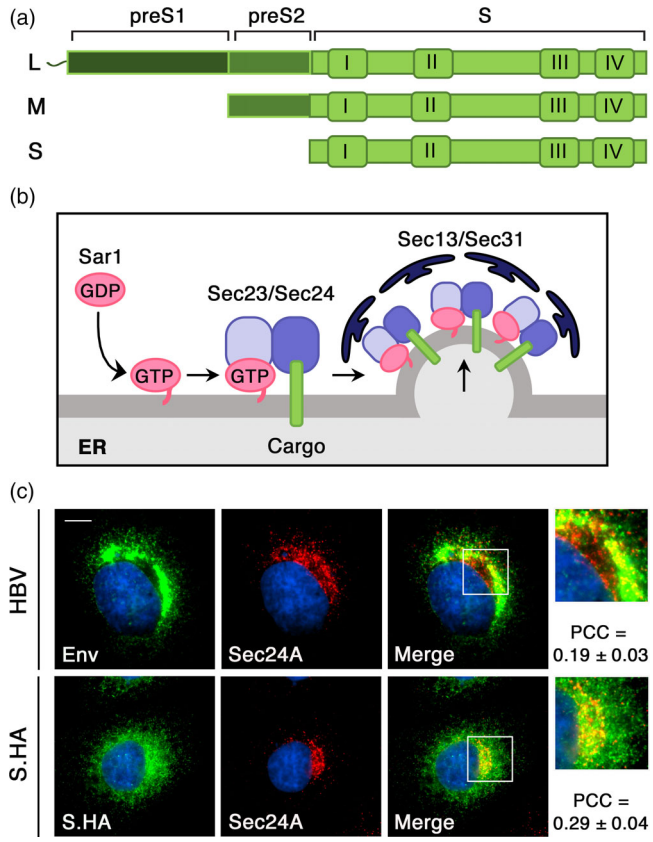

FIGURE 1 The hepatitis B virus (HBV) envelope is an interaction partner of Sec24A. (a) Domain structures of the L, M, and S proteins. Due to the usage of a single open reading frame (ORF), all three proteins contain the S domain (light green) consisting of 226 aa. The M protein is N-terminally extended for the preS2 domain (medium green) encoding for 55 aa. The L protein carries in addition the N-terminal preS1 domain (dark green) consisting of 108 or 119 aa, depending on genotype. The predicted four transmembrane I, II, III, and IV segments of the S domain are highlighted. (b) Schematic diagram of the vesicle budding process of the coat protein complex II (COPII) complex at endoplasmic reticulum (ER) export sites. GTP activation of Sar1 by a guanine nucleotide exchange factor leads to membrane recruitment and formation of a Sec23/24 heterodimer complex, cargo selection, and coat polymerization by the Sec13/31 complex. (c) Colocalization of the HBV envelope proteins and Sec24A in human liver cells. HuH-7 cells were transfected with the pHBV replicon construct (HBV, top) or an hemagglutinin (HA)-tagged version of HBV S (S.HA, bottom). Three days post transfection, cells were fixed, permeabilized, and reacted with either mouse antibodies against the S domain (top, green) or mouse anti-HA antibodies (bottom, green) and rabbit anti-Sec24A (red) antibodies. Thereafter, cells were stained with Alexa_Fluor® 488-conjugated anti-mouse and Alexa_Fluor® 546-conjugated anti-rabbit antibodies. DNA staining is shown in blue. Overlaid staining patterns are displayed in the Merge panels with outlined areas showing enlargements. Bar, 10 μm. For quantitative colocalization analysis (QCA), Pearson correlation coefficient (PCC) values were calculated and represent the mean ± *SD*

isoform (aa 1–613) of human Sec24A (NM_021982) was purchased from the RZPD (Deutsches Ressourcenzentrum für Genomforschung). The Sec24A gene was inserted into plasmid pCMV-Myc (Clontech) or p3xFLAG-CMV-10 (Sigma-Aldrich) via PCR-directed cloning to generate a N-terminal Myc- or FLAG-tagged version, respectively. The expression vector pcDNA3.1(+)-N-Myc-Sec24A encoding the long Sec24A isoform (NM_021982.2; aa 1–1093) with an N-terminal Myc-tag was purchased from GenScript. A plasmid carrying the human Sar1A cDNA (NM_01142648) was purchased from Origene and used to subclone the Sar1A gene into pCMV-Myc (Clontech). All constructs were verified by sequencing, and cloning details are available on request.

2.2 | Antibodies

To detect the S protein under native conditions, a rabbit polyclonal antiserum (K38; Loffler-Mary, Dumortier, Klentsch-Zimmer, & Prange, 2000) or a mouse antibody (HepBsAg, sc-53300, Santa Cruz) raised against recombinant HBV SVP particles was used. For immunodetection of the L protein, a rabbit antibody raised against a recombinant peptide encoding aa 1–42 of L fused to glutathione *S*-transferase was employed (K1350; Eurogentec). The mouse anti-ERGIC-53 (sc-365158) and anti-Sec31A (sc-376587) antibodies were purchased from Santa Cruz. Antibodies obtained from Covance were mice anti-HA (16B12) and anti-Myc (9E10). Antibodies obtained from Sigma-Aldrich were anti-Sec24A (HPA056825), anti-FLAG (F3165), and anti-β-actin (AC15). Rabbit antibodies directed against Sec24B (D7D6S), Sec24C (D9M4N), and Sec24D (D9M7L) were purchased from Cell Signaling. Peroxidase-labeled secondary antibodies were obtained from Dianova, and fluorophore-labeled antibodies were purchased from Thermo Fisher Scientific.

2.3 | SiRNAs, cell culture, and transfection

The human hepatocellular carcinoma cell line HuH-7 was obtained from the Japanese Collection of Research Bioresources. The HepG2 cell line was bought from the American Type Culture Collection; and the HepG2.2.15 cell line, which persistently produces HBV due to the integrated HBV genome, was kindly provided by Dr. P. Gerner (University Medical Center, Mainz, Germany). Cells were cultured in Dulbecco's modified Eagle's medium supplemented with 10% fetal bovine serum and 5 μg ml^{-1} of ciprofloxacin. Transfections of HuH-7 cells with plasmid DNAs were performed with LipoFectamine™ Plus (Thermo Fisher Scientific). To transfect cells with siRNAs, the LipoFectamine™ RNAiMAX transfection reagent (Thermo Fisher Scientific) was utilized. Briefly, 5×10^5 cells per well of a 6-well plate were transfected with a final concentration of 20 nM of siRNA according to the protocol of the supplier. After 48 to 72 h, cells were retransfected with 4 μg of plasmid DNA using LipoFectamine™ Plus (Thermo Fisher Scientific), and transfected cells were harvested after additional 24 to 72 h, as indicated in the figure legends. The sequences of the siRNA oligos are listed in Table S1 and were obtained from Dharmacon and Sigma-Aldrich. For drug treatment, cells were incubated with 1 μM of brefeldin A (BFA; Sigma-Aldrich) at 37°C for 2 to 18 h, as indicated in the figure legends.

2.4 | Quantitative reverse transcription PCR analysis

Total mRNAs were isolated from cells using the preqGold TriFast (Peqlab Biotechnologie) and the Direct-zol™ RNA MiniPrep kit (Zymo Research), according to the protocols of the suppliers. The mRNA was treated with 5 U of RNase-free, recombinant DNase I (Hoffmann-La Roche), and cDNA synthesis was performed by using the qScript cDNA Synthesis Kit (Quanta BioSciences). Quantitative reverse transcription PCR (qRT-PCR) reactions were performed as described (Doring et al., 2018). For data analysis, the comparative cycle threshold method (C_T) was used, and data were reported as the fold change normalized to an endogenous reference gene (β-actin). Primer pairs are listed in Table S2 and were purchased Thermo Fisher Scientific and Sigma-Aldrich.

2.5 | Cell lysis, cell supernatant analysis, and enzyme-linked immunosorbent assay

To probe for protein expression, cells were lysed with Nonidet P-40 (NP-40) in Tris-buffered saline (50 mM of Tris–HCl pH 7.5, 150 mM of NaCl, 0.5% NP-40) for 20 min on ice, and lysates were centrifuged for 5 min at 15,000×g and 4°C. To analyse the assembly and release of SVPs from transfected cells, clarified culture medium was concentrated by ultracentrifugation through a 20% (w/v) sucrose cushion (4 h at 100,000×g and 4°C), and pellets were suspended in Laemmli buffer. Lysates and concentrated supernatants were subjected to SDS-PAGE and Western blotting (WB) analyses using standard procedures. The synthesis and release of the HBV envelope proteins or the HBV preC protein were assayed with the Murex HBsAg Version 3 kit (DiaSorin) or the ETI-EBK PLUS enzyme-linked immunosorbent assay (ELISA) kit (DiaSorin), respectively. The secretion of AFP by the HuH-7 cells was measured by an AFP-specific ELISA (Demeditec Diagnostics).

2.6 | Fluorescence microscopy

For immunofluorescence (IF), cells grown on coverslips were fixed with 4% paraformaldehyde (PFA) for 10 min at room temperature and permeabilized with 0.2% Triton X-100 for 10 min at room temperature. Cells were blocked in PBS containing 1% BSA, incubated with the indicated primary antibodies for 1 h at 37°C, rinsed with PBS, and then incubated with Alexa_Fluor®-tagged secondary antibodies (Thermo Fisher Scientific) for 1 h at 37°C. Cell nuclei (DNA) were stained with Hoechst 33342 (Sigma-Aldrich). Images were acquired separately for each channel using a Zeiss Axiovert 200M microscope equipped with a Plan-Apochromat 100× (1.4 NA) and a Zeiss Axiocam digital camera. AxioVision software 4.7.1 was used for merging pictures, and Tiffs were assembled into figures using Adobe Photoshop CS6. For quantitative colocalization analysis, digital photographs were quantitated using the AxioVision colocalization software (4.7.1) by calculating the pixel intensity-based Pearson correlation coefficients of randomly selected cells (25 cells per coverslip).

2.7 | Coimmunoprecipitation assay

To probe for complex formation, cells were lysed with RIPA buffer (50 mM of Tris–HCl, pH 7.5, 150 mM of NaCl, 1 mM of EDTA, 1% NP-40, 0.5% deoxycholate, supplemented with 1× protease inhibitor mixture) for 20 min on ice. After centrifugation for 20 min at 15,000×g and 4°C, lysates were immediately subjected to immunoprecipitation using tosyl-activated, superparamagnetic polystyrene beads (Dynabeads Sheep anti-rabbit IgG; DYNAL, Thermo Fisher Scientific) that had been precoated with the anti-S antibody K38 as described (Rost et al., 2006). After incubation for 3 h at 4°C with agitation, the immune complexes were washed three times with 50 mM of Tris–HCl, pH 7.5, 150 mM of NaCl, 1% NP-40, and 0.5% deoxycholate and once with PBS.

2.8 | Image analysis

Densitometry analysis of Western blots was performed using the ImageJ software of the National Institutes of Health (https://imagej.nih.gov/ij/).

2.9 | Statistical analysis

Statistical differences between groups and statistical graphs were assessed with a two-tailed, unpaired *t*-test using Microsoft Office Excel 2016. Differences between groups were considered significant when the *p* value was $^{*}p < .05$ or $^{**}p < .01$.

3 | RESULTS

3.1 | A split-ubiquitin based membrane Y2H analysis and in situ colocalization studies reveal HBV envelope interaction with Sec24A

The HBV envelope proteins are expressed by a single ORF with three different start codons and a common stop codon. Consequently, the amino acid (aa) sequence of S is repeated at the C-termini of M and L that carry the additional preS2 domain or preS1 plus preS2 domains, respectively (Figure 1a). All three proteins are cotranslationally integrated into the ER membrane, giving rise to multispanning transmembrane (TM) proteins that are ultimately transported to subviral and viral particle assembly sites (Blondot et al., 2016; Hu & Seeger, 2015; Prange, 2012). To identify unknown host factors involved in the maturation and intracellular transport of the envelope proteins, our lab employed a split-ubiquitin based Y2H assay using the HBV envelope proteins as baits and proteins encoded by a human cDNA library as

preys. This assay led to the identification of Sec24A, a cargo adaptor of the COPII machinery (Figure 1b), that interacted with both L and S and thus with the S domain of the HBV envelope proteins (Awe, 2009).

Next, we attempted to demonstrate interplay between the viral S domain and Sec24A under natural settings by using the human hepatoma cell line HuH-7 that is permissive for HBV replication. To visually examine an interaction of the S domain with Sec24A, we inspected their intracellular localization in HBV-replicating HuH-7 cells. Cells were transiently transfected with an HBV replicon plasmid, fixed with PFA, permeabilized with Triton X-100, and stained with anti-S domain and anti-Sec24A antibodies. The staining of the envelope proteins resulted in a granular labeling along with a perinuclear accumulation, typical for viral surface proteins that are synthesized at the ER (Figure 1c). Sec24A yielded a punctuated staining pattern in the perinuclear region with some subcellular accumulations, likely occurring at ERES (Figure 1c). Importantly, the overlays of the fluorescence patterns revealed a significant degree of colocalization of the envelope proteins and Sec24A, indicative for close contacts between the S domain and Sec24A during HBV propagation in hepatocytes. Similar degrees of colocalization between S and Sec24A were observed in cells solely expressing S without an ongoing virus replication (Figure 1c). To this end, HuH-7 cells were transfected with a plasmid encoding S with a C-terminally tagged HA epitope (S.HA) under the transcriptional control of the human hMT IIA promoter. It is worth noting that previous studies have shown that the addition of the HA-tag did not alter the natural features of S (Lambert, Thome, Kluck, & Prange, 2004). In this setting, cells were costained with anti-HA and anti-Sec24A antibodies. Collectively, the Y2H and IF data indicate that Sec24A is a putative host factor contacting the S domain of the HBV envelope in both the presence and absence of an ongoing virus replication.

3.2 | HBV SVP secretion requires Sec24A

Accordingly, we first investigated whether an interference with Sec24A functions may affect HBV envelope formation and egress. For RNA interference (RNAi), cells were treated with control siRNAs or a siRNA pool containing four different duplexes targeting Sec24A for 72 h prior to transfection with the pHBV replicon. After an additional 48 h, cell lysates and supernatants were harvested. The analysis of lysates by Sec24A-specific WB revealed an efficient knockdown (KD) of Sec24A (Figure 2a), which was confirmed by an additional qRT-PCR analysis of Sec24A transcript levels (see Figure S2a). Intracellular and extracellular HBV envelope protein levels were analysed by an HBsAg-specific ELISA that recognizes a conformational epitope shared by the three S, M, and L proteins. The silencing of Sec24A significantly reduced the extracellular pool of viral envelopes as compared with control cells and concomitantly increased intracellular envelope levels (Figure 2a). These results first indicated a functional role of Sec24A in HBV envelope trafficking and egress.

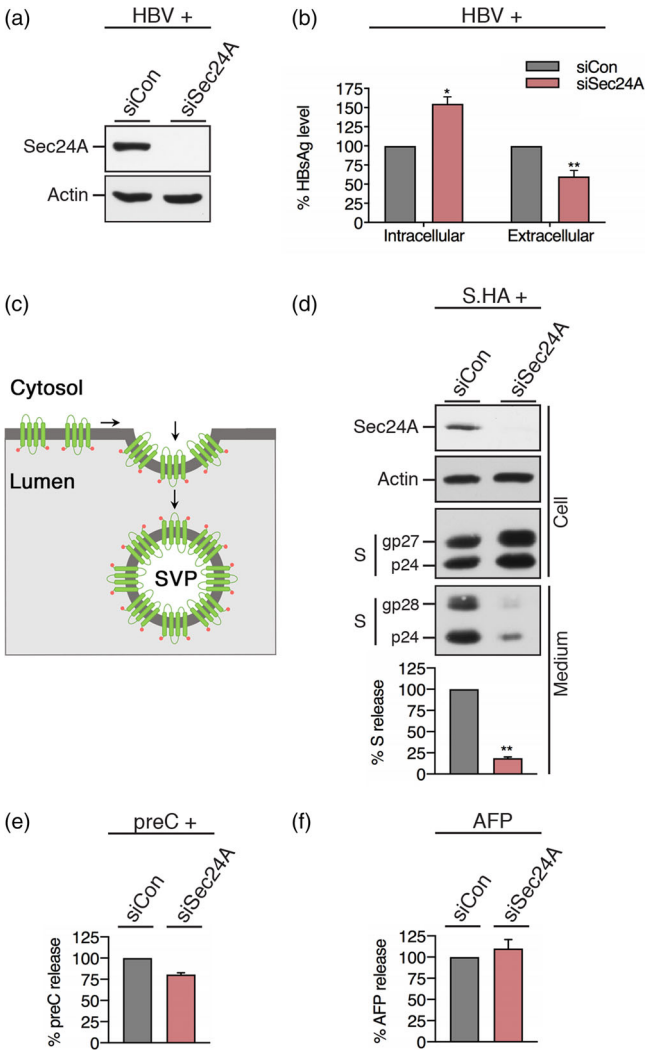

FIGURE 2 Hepatitis B virus (HBV) S envelope protein secretion requires Sec24A. (a) Treatment of HuH-7 cells with control (siCon) or a Sec24A-specific siRNA pool for 3 days and retransfection with the pHBV replicon construct for an additional 2 days. To monitor depletion, cell lysates were examined by Sec24A- and β-actin-specific Western blotting (WB) (left). Intracellular and extracellular HBV envelope protein levels were determined by probing of cell lysates and supernatants, respectively, with an HBsAg-specific enzyme-linked immunosorbent assay (ELISA; right; $n = 3$, ±*SD*). (b) Model for HBV subviral envelope particle (SVP) morphogenesis. The S envelope protein is synthesized at the endoplasmic reticulum (ER) membrane where its predicted four TM segments project its N- and C-terminus (depicted by purple dots) into the ER lumen. Following dimerization/oligomerization of S chains, spherical SVPs bud into the lumen of secretory organelles. (c) HuH-7 cells were treated with the indicated siRNAs as above and retransfected with the hemagglutinin (HA)-tagged S construct (S.HA) for 2 days. Cell lysates (Cell) were examined by Sec24A-, β-actin, and HA-specific WB, and concentrated cell supernatants (Medium) were probed by anti-HA immunoblotting. The nonglycosylated (p24) and glycosylated (gp27 and gp28) forms of S.HA are depicted. The degree of extracellular S.HA release was quantified by densitometric analysis of Western blots and demonstrated in percent amount relative to control cells ($n = 3$, ±*SD*). (d, e) Cells were treated with the indicated siRNAs and retransfected with an HBV preCore expression construct (preC; d) or left untransfected (e). For quantification of preC and AFP secretion, cellular supernatants were assayed by specific ELISAs. Data are representative of two (d) or three (e) independent experiments (± *SD*)

Despite their similarities, the three HBV envelope proteins differ in functions. The L protein is essential for viral particle production and infectivity as it mediates capsid envelopment and bile acid transporter sodium taurocholate cotransporting polypeptide receptor binding, respectively (Bruss, 1997; W. Li, 2015). The M protein is required for neither viral nor subviral particle formation, whereas the S protein builds up the scaffold of the viral and subviral envelope. The S protein alone is sufficient for the production and secretion of SVPs, defined lipoprotein complexes that are formed by self-assembly and intraluminal budding of about 96 transmembrane S molecules in the secretory system (Figure 2b). SVPs are secreted in large excess compared with the number of mature HBV virions and are thought to leave the cell via the constitutive pathway of secretion (Blondot et al., 2016; Huovila, Eder, & Fuller, 1992; Patient, Hourioux, & Roingeard, 2009; Prange, 2012). Inspired by the aforementioned results, we thus investigated whether Sec24A might play a role in HBV SVP formation and secretion. For this purpose, we employed an SVP release assay and transiently transfected HuH-7 cells with the expression construct encoding the HA-tagged S gene (S.HA) and examined the intracellular and extracellular S.HA levels by HA-specific WB. For RNAi, cells were treated with control or Sec24A-specific RNA duplexes as above (72 h) prior to transfection with S.HA (48 h). Thereafter, cell lysates and supernatants were harvested, and SVPs present in the supernatants were collected by ultracentrifugation through sucrose cushions. The inspection of the intracellular and extracellular S.HA levels by HA-specific WB showed that the depletion of Sec24A did not interfere with the synthesis and the typical partial N-glycosylation of S.HA, a convenient marker for its proper integration into the ER membrane. However, Sec24A silencing strongly inhibited the extracellular release of S.HA as compared with control cells and concomitantly increased intracellular S.HA levels (Figure 2c). An inhibition of SVP secretion was also observed when a single Sec24A-specific siRNA unrelated to the pool was used, which led us to exclude off-targeting effects of the applied siRNA strategy (Figure S1a). Likewise, when S.HA synthesis was driven by the authentic HBV S promoter rather than the foreign hMT IIA promoter, SVP secretion dropped down upon Sec24A silencing (Figure S1b), thereby excluding artificial results due to ectopic S.HA overexpression.

To preclude the possibility that a functional loss of Sec24A may generally impair the secretory pathway of the HuH-7 cell line, the secretion profile of two soluble proteins was monitored. As reporters, we analysed the degree of secretion of the HBV preC protein, a secretory variant of the viral core protein, and alpha-fetoprotein (AFP), a soluble protein known to be secreted from hepatocarcinomic cells. Control and Sec24A-depleted cells were retransfected with a preC expression construct or were left untransfected, and cellular supernatants were probed by preC- and AFP-specific ELISAs, respectively. The inactivation of Sec24A had no significant impacts on the extracellular release of ectopically expressed preC (Figure 2d) or endogenously synthesized AFP (Figure 2e), therefore suggesting no misfunction of the cellular secretory pathways due to loss of the COPII component.

3.3 | HBV SVP secretion selectively requires the Sec24A isoform

Besides Sec24A, mammalian cells express three other paralogs termed Sec24B, Sec24C, and Sec24D that share 53%, 30%, and 28% aa identity with Sec24A (Wendeler, Paccaud, & Hauri, 2007). The results shown in Figure 2 implicated that the Sec24B, Sec24C, and Sec24D isoforms were seemingly unable to substitute for the functional loss of Sec24A in HBV SVP secretion. For proof of principle, each of the four Sec24 isoforms was individually depleted in HuH-7 cells prior to transfection with the S.HA expression plasmid. Of note, the

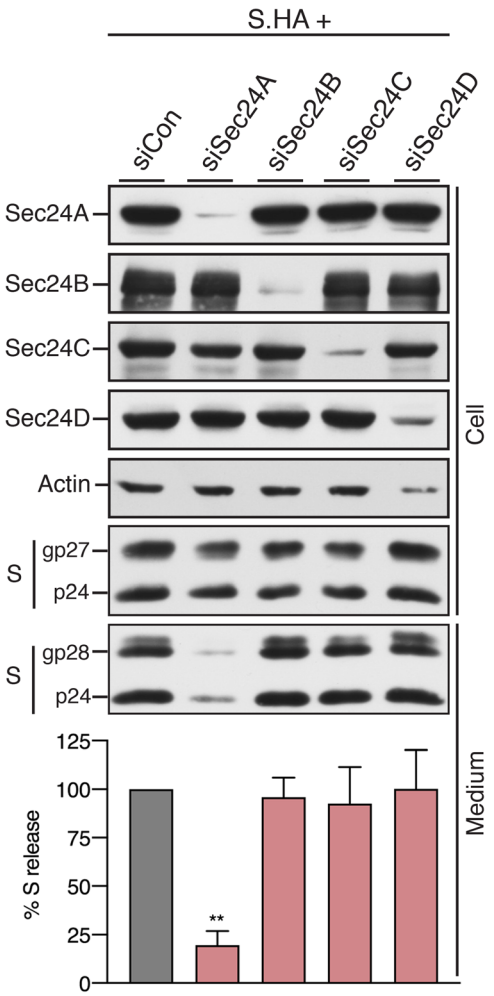

FIGURE 3 The hepatitis B virus (HBV) S envelope protein is a specific client of Sec24A. (a) For individual depletion of the four Sec24 isoforms, HuH-7 cells were treated with the indicated siRNAs or siCon duplexes for 2 days and retransfected with S.HA for 1 day. Cell lysates (Cell) were subjected to immunoblotting using antibodies against Sec24A, Sec24B, Sec24C, Sec24D, β-actin, and the hemagglutinin (HA)-tag, as indicated in the left of the panels. Extracellular (Medium) proteins were probed by HA-specific Western blotting (WB) and a representative blot is shown. The p/gp forms of S. HA are indicated. The degree of S.HA release was quantified by densitometric analysis of Western blots and demonstrated in percent amount relative to control cells (n = 3, ±*SD*)

transfection scheme was modified here in such that RNA transfection proceeded for 48 h followed by a 24-h DNA transfection period. To analyse the KD efficiency of the applied siRNAs, cellular lysates were subjected to WB analysis using Sec24 isoform-specific antibodies. Each siRNA reduced the expression of its specific target without affecting the protein levels of the related Sec24 paralogs (Figure 3). The potency of the siRNAs and the absence of apparent codepletion effects were confirmed by qRT-PCR analysis of total cellular RNA using Sec24 isoform-specific primer pairs (Figure S2a, b). HA-specific WB analysis of lysates and supernatants demonstrated that the depletion of Sec24A, but not of the related Sec24B, Sec24C, and Sec24D isoforms, reduced the secretion of S.HA (Figure 3). In contrast to the results shown in Figure 2a, a concomitant intracellular accumulation of S.HA in Sec24A KD cells was less evident likely as a consequence to the shortened time frame of DNA transfection. However, upon an extension of the transfection frame, again, a substantial intracellular accumulation of S.HA in Sec24A-silenced cells could be observed (Figure S2c). Given that even the closely related Sec24B paralog is unable to compensate for Sec24A function in S.HA secretion, we deduce that the HBV S protein is a selective client of the Sec24A isoform.

3.4 | HBV SVP secretion requires Sar1

The observed isoform specificity prompted us to analyse next whether Sec24A may govern S.HA secretion either alone or in conjunction with other COPII components. First, we focused on the Sar1 GTPase that initiates COPII coat assembly by binding to ER membranes in its GTP-loaded form, thereby recruiting the heterodimeric complex of Sec23 and Sec24 (Barlowe & Helenius, 2016; Bethune & Wieland, 2018; Miller & Schekman, 2013). Human cells encode two Sar1 isoforms, Sar1A and Sar1B, that share 89% sequence identity with reportedly overlapping functions in the secretory system (Wang et al., 2018). For RNAi, a Sar1A-specific siRNA pool or a Sar1B-specific single siRNA were transfected into HuH-7 cells either individually or in combination. After 48 h, cells were retransfected with S.HA and harvested 24 h later. The measurement of Sar1-specific transcripts by qRT-PCR revealed an almost complete KD upon the individual depletion of either isoform (Figure 4). In case of Sar1A, we found that the transcriptional repression coincided with reduced protein levels (Figure 4). Under these conditions, the secretion of S.HA was only marginally affected. Conversely, the combined depletion of Sar1A and Sar1B led to a virtual complete block in extracellular S.HA release (Figure 4), indicating that S export requires functional Sar1, provided by either Sar1 isoform, and hence a Sar1-mediated recruitment of COPII coat components.

3.5 | HBV SVP secretion selectively requires the Sec23B isoform

All of the Sec24 isoforms are known to act in concert with Sec23 during COPII coat assembly and cargo sorting. Similar to Sar1, mammals contain two Sec23 paralogs, Sec23A and Sec23B, that are highly similar in sequence (84% identity) and function (Khoriaty et al., 2018). To investigate their impacts on S secretion, Sec23A and Sec23B were individually depleted from S.HA-producing HuH-7 cells using isoform-specific, single siRNA duplexes. As evaluated by qRT-PCR analysis, both siRNAs effectively reduced the transcript levels of their targets (Figure 5a). For a validation on the protein level, we tested two commercially available anti-Sec23B antibodies, which, however, failed to work (data not shown). Whereas the functional loss of Sec23A had only a slight inhibitory effect on the secretion of S.HA, the

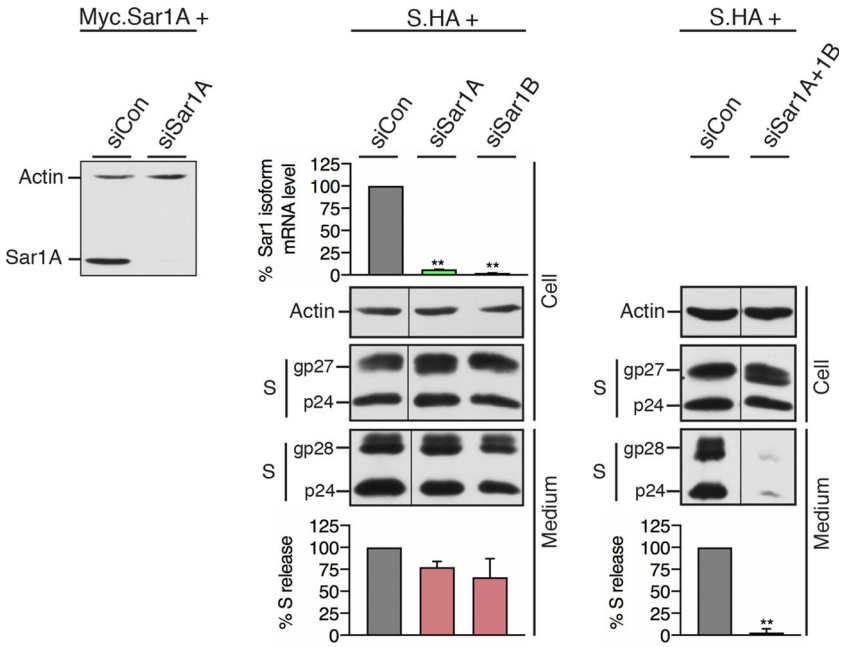

FIGURE 4 Hepatitis B virus (HBV) S envelope protein secretion depends on Sar1. Treatment of HuH-7 cells with siCon-, siSar1A-, or Sar1B-specific siRNAs (2 days) either individually or together, as denoted above each lane, prior to retransfection with S.HA or a Myc-tagged version of Sar1A (1 day). Depletion efficiencies of Sar1A and Sar1B were analysed by quantitative reverse transcription PCR (qRT-PCR) analysis of total cellular RNA. Data are representative of two independent experiments measured in duplicate (± *SD*). To detect Sar1A silencing on the protein level, cell lysates were probed by β-actin- and Myc-specific Western blotting (WB) (left). For HBV S protein analyses, cellular extracts (Cell) and supernatants (Medium) were probed by β-actin- and hemagglutinin (HA)-specific immunoblotting (middle, right). The p/gp forms of S.HA are indicated. For quantification of S.HA secretion, Western blots were subjected to densitometric analysis and demonstrated in percent amount relative to control cells (n = 2, ±*SD*)

inactivation of the Sec23B isoform significantly reduced the extracellular release of S.HA (Figure 5a). In respect to the reported overlapping functions of the two Sec23 paralogs (Khoriaty et al., 2018), the unique requirement of S.HA for Sec23B and the limited compensation capability of Sec23A for Sec23B silencing during S trafficking were surprising observations.

Finally, we performed loss-of-function assays to investigate the role of the heterotetrameric Sec13/Sec31 complex, scaffolding the COPII coat as an outer layer. However, the individual depletion of Sec13 from HuH-7 cells with two different siRNAs turned out to be harmful and dramatically inhibited S synthesis (data not shown), likely because human cells express only one Sec13 isoform. In case of Sec31, we succeeded to deplete the Sec31A isoform, whereas RNAi experiments targeting Sec31B remained unsuccessful. Nonetheless, the reduction of Sec31A expression by about 80%, as evidenced by qRT-PCR and WB analyses, resulted in a bisection of extracellular

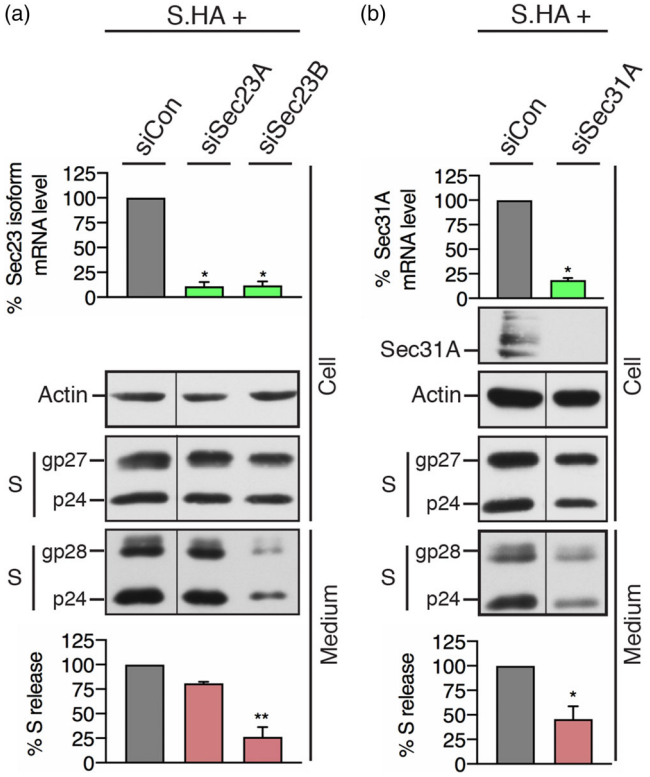

FIGURE 5 Hepatitis B virus (HBV) S envelope protein secretion requires Sec23B. (a) For RNAi, HuH-7 cells were transfected with siCon-, siSec23A-, or siSec23B-specific RNA duplexes (2 days) followed by DNA transfection with the hemagglutinin (HA)-tagged S gene (1 day). To check for depletion, transcript levels of Sec23A and Sec23B were measured by quantitative reverse transcription PCR (qRT-PCR) and demonstrated in percent amount relative to control cells (n = 2, ±*SD*). Cellular lysates (Cell) and supernatants (Medium) were subjected to β-actin- and HA-specific Western blotting (WB). The p/gp forms of S.HA are indicated. The degree of S.HA secretion was quantified by densitometric analysis of Western blots (n = 2, ±*SD*). (b) For silencing of Sec31A, cells were treated with specific RNA oligos. The subviral envelope particle (SVP) release assay and qRT-PCR analysis were done as in (a) except for WB analysis of lysates with Sec31A-specific antibodies

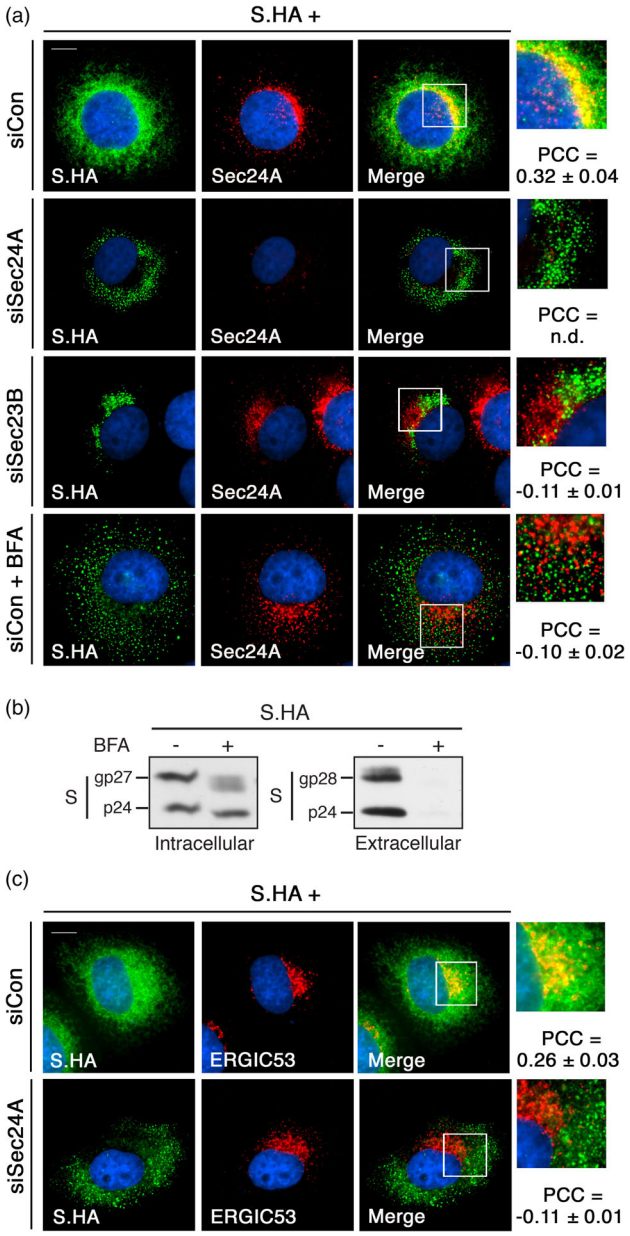

FIGURE 6 Silencing of Sec24A and Sec23B blocks endoplasmic reticulum (ER) export of hepatitis B virus (HBV) S. (a) HuH-7 cells were treated with siCon (top and bottom), siSec24A (top middle), or siSec23B (bottom middle) duplexes for 2 days and retransfected with S.HA. Four days post transfection, cells were fixed with paraformaldehyde (PFA) and permeabilized. Where indicated (bottom panel), cells were incubated with brefeldin A (BFA) for 2 h prior to fixation. Cells were stained with hemagglutinin (HA)- (green) and Sec24A-specific (red) antibodies. DNA staining is shown in blue. Overlaid images of S.HA and Sec24A staining (yellow) are displayed in the Merge panels. Outlined areas are shown at larger magnifications. Bar, 10 μm. For quantitative colocalization analysis (QCA), Pearson correlation coefficient (PCC) values were calculated and represent the mean ± *SD*. (b) S.HA-expressing HuH-7 cells were either mock-treated or treated with BFA for 18 h, and cell lysates (Intracellular) and concentrated cell supernatants (Extracellular) were probed by HA-specific Western blotting (WB). The p/gp forms of S.HA are indicated. (c) Treatment of HuH-7 cells with siCon- (top) or Sec24A-specific (bottom) siRNAs (2 days) prior to retransfection with pNI2.S.HA (2 days). After fixation and permeabilization, cells were reacted with antibodies against HA (green) and ERGIC-53 (red). Nuclei staining is shown in blue. Bar, 10 μm

S.HA levels as compared with control cells (Figure 5b). Collectively, our results are pointing towards a requirement of the complete COPII machinery in HBV SVP secretion with an exceptional need for Sec24A/Sec23B.

3.6 | Sec24A/Sec23B silencing blocks ER export of HBV S

To study the fate of HBV S upon COPII inactivation in single cells, IF studies were performed. HuH-7 cells were treated with control and Sec24A- and Sec23B-specific siRNAs, retransfected with HA-tagged S, and stained with HA and Sec24A antibodies. As shown above, S showed a diffuse granular intracellular labeling in the control cells, as presumed for a protein that is transported through the secretory pathway. Endogenous Sec24A yielded a punctate pattern with local accumulations, likely occurring at ERES, where it strongly colocalized with S.HA (Figure 6a). As expected, the Sec24A signals got lost in siSec24A-treated cells but remained unimpaired in siSec23B-transfected cells. Importantly, upon Sec24A or Sec23B depletion, the staining pattern of S.HA strongly changed, as it now appeared in dot-like structures, reminiscent of vesicular aggregates (Figure 6a). Of note, these S.HA microdots no longer colocalized with Sec24A in Sec23B-depleted cells, suggesting their inaccessibility for Sec24A. A similar emergence of dot-like S.HA structures was found when S.HA-expressing cells were treated with BFA (Figure 6a). BFA is an established fungal compound that inhibits protein trafficking and secretion in mammalian cells via targeting the formation of COPI-coated vesicles that are responsible for retrograde protein transport from the Golgi to the ER. The disruption of the COPI route by BFA in turn leads to the collapse of ER export, as COPI vesicles are needed for the proper organization of ERESs (Nebenfuhr, Ritzenthaler, & Robinson, 2002). To verify the inhibitory action of BFA on S export, S.HA-expressing cells were treated in the absence or presence of the drug and subjected to the SVP assay. As shown in Figure 6b, BFA completely blocked S.HA secretion into the extracellular space. Because the BFA treatment pheno-copied the Sec24A/Sec23B phenotypes, S is likely discharged from ER exit when these COPII components are missing. For verification, we analysed the subcellular localization of the punctate S.HA structures by labeling of cells with anti-HA antibodies and an antibody against ERGIC-53, a known marker of the ER-Golgi intermediate compartment (ERGIC). In control cells, S.HA largely colocalized with the ERGIC53-stained structures, whereas no fluorescence overlap could be observed in Sec24A-KD cells (Figure 6c). We infer from these results that the loss of Sec24A/Sec23B blocked the transport of S.HA out of the ER into the ERGIC akin to the action of BFA. The imposed ER export block of S.HA may trigger the emergence of the aberrant, dot-like S.HA structures.

To corroborate the dispensability of the Sec24B/C/D and Sec23A isoforms in HBV S trafficking and secretion, comparable IF analyses were performed in correspondingly KD cells. Upon cell labeling with HA-specific antibodies, S.HA exhibited its typical intracellular distribution that was entirely congruent with the staining pattern of siCon-treated cells (Figure 7). Moreover, S.HA colocalized with Sec24A irrespective of whether Sec24B/C/D or Sec23A was depleted or not (Figure 7). Hence, these COPII components are dispensable for normal HBV S trafficking.

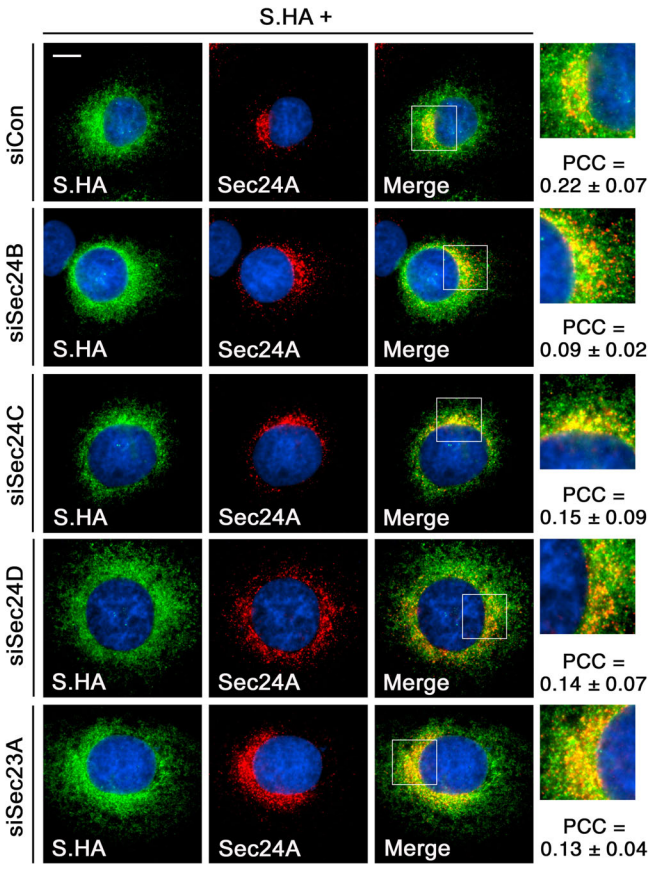

FIGURE 7 Silencing of Sec24B/C/D or Sec23A did not alter the intracellular distribution of hepatitis B virus (HBV) S. HuH-7 cells were treated with the indicated siRNAs (2 days) and retransfected with S.HA (2 days) prior to processing for immunofluorescence (IF) analysis. Cells were reacted with hemagglutinin (HA)- (green) and Sec24A-specific (red) antibodies. DNA staining is shown in blue. Overlaid pictures (yellow) are displaced in the Merge panels with outlined areas showing larger magnifications. Bar, 10 μm. For quantitative colocalization analysis (QCA), Pearson correlation coefficient (PCC) values were calculated and represent the mean ± *SD*

3.7 | Mapping analyses reveal an interaction of the N-terminal half of Sec24A with a di-arginine motif of the HBV envelope

Collectively, our results suggested a functional interaction between HBV S and Sec24A. Mammalian cells express not only the four Sec24 paralogs but even a short isoform and a long isoform of Sec24A itself, derived from alternative splicing. This prompted us to construct expression plasmids encoding its long (Sec24A.1093; briefly, Sec24A.l) or short (Sec24A.613; briefly, Sec24A.s) isoforms fused with N-

terminal Myc-tags. Upon expression in HuH-7 cells, Myc.Sec24A.l and Myc.Sec24A.s were synthesized in 120- and 68-kDa forms, respectively, which is consistent with their calculated molecular masses (Figure 8a). Immunostaining of cells cotransfected with S.HA and Myc.Sec24A.l or Myc.Sec24A.s showed that both Sec24A forms yielded a punctuated staining pattern with some fraying, occurring in cells that expressed the short Sec24A form. Intriguingly, both forms colocalized with S.HA (Figure 8a), implicating that the N-terminal half of Sec24A (i.e., aa 1 to 613) is sufficient to establish contact sites with S.

To corroborate these results, we next performed coimmunoprecipitation (CO-IP) analyses. HuH-7 cells were cotransfected with Myc.Sec24A.s and S.HA, and lysates were subjected to an S-specific IP followed by Myc-specific WB. Thereby, S.HA reproducibly brought down Myc.Sec24A.s (Figure 8c), thus demonstrating a physical interaction between S.HA and Sec24A involving the N-terminal half of the COPII cargo adaptor. In principal, the four Sec24 paralogs recognize ER export motifs of cargo proteins on the cytosolic side of the ER membrane (Barlowe & Helenius, 2016; Bethune & Wieland, 2018; Miller &

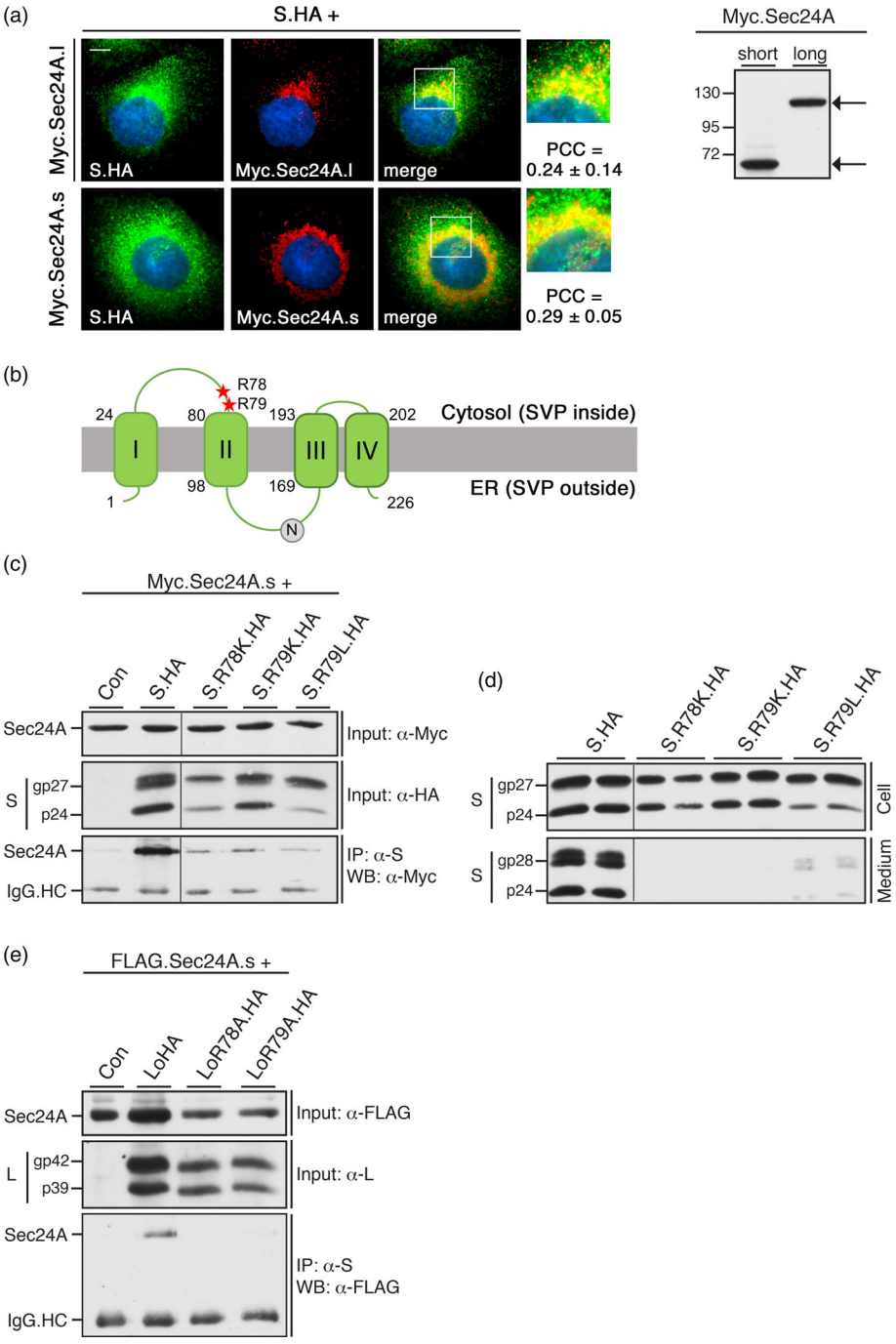

FIGURE 8 Legend on next page.

Schekman, 2013; Wendeler et al., 2007). According to the model for the transmembrane topology of the S monomer at the ER membrane (Prange, 2012; Stirk, Thornton, & Howard, 1992; Suffner et al., 2018), we suspected its two cytosolic loops as candidate binding regions for Sec24A (Figure 8b). Because previous deletion analyses had shown that residues including the second cytosolic loop (i.e., aa 172 to 226) are dispensable for S assembly and secretion (Suffner et al., 2018), we focused on the first cytosolic loop connecting TM segments I and II. Intriguingly, this loop is terminated by two consecutive arginine residues (R78 and R79) that partly resemble known dibasic ER export motifs (Dong et al., 2012). Therefore, we analysed the properties of S.HA mutants in which R78 or R79 was substituted by lysine and leucine residues. Upon cotransfection with Myc.Sec24A.i and immunoprecipitation analyses, all three S.R78K, S.R79K, and S.R79L mutants failed to effectively associate with Sec24A (Figure 8c). In line with this, we found that all three S mutants were blocked in secretion despite their proper synthesis/stability and N-linked glycosylation (Figure 8d). We thus deduce that the cytosolically exposed, dibasic R78/R79 module of S comprises a binding site required for a productive interaction with Sec24A and hence for ER export and secretion of HBV SVPs.

Finally, we analysed the Sec24A-interacting properties of the HBV L envelope protein that is essential for viral particle formation. Unlike S, L adopts a dual transmembrane topology by disposing its N-terminal preS domain to both the luminal and cytosolic sides of the ER membrane (Prange, 2012). Accordingly, the conformation of the first hydrophilic loop with the dibasic R78/R79 motif may differ between L and S. For CO-IP analysis, cells were cotransfected with FLAG.Sec24A.s and an L_OHA construct that exclusively drives L expression without concomitant S and M envelope protein synthesis (Lambert, Mann, & Prange, 2004). Lysates were subjected to an S domain-specific IP followed by FLAG-specific WB. Thereby, L_OHA, synthesized in nonglycosylated p39 and glycosylated gp42 forms, clearly co-precipitated FLAG.Sec24A.s (Figure 8e). Under the same conditions, L_OHA mutants carrying alanine substitutions within the R78/R79 module failed to bring down FLAG.Sec24A.s (Figure 8e). These data implicate that L protein trafficking and possibly viral particle egress may likewise depend on Sec24A.

3.8 | HBV replication upregulates Sec24A and Sec23B gene transcription

Because Sec24A/Sec23B-guided processes are pivotal for HBV, we next investigated whether HBV replication had an effect on the expression of these proviral COPII components. HuH-7 cells were transiently transfected with an empty plasmid backbone or the pHBV replicon for 3 days. For gene expression profiling, total mRNA was isolated and subjected to qRT-PCR with Sec24A- or Sec23B-specific primer pairs. As shown in Figure 9, HBV replication significantly upregulated Sec24A and Sec23B transcription as compared with control cells. For corroboration in another hepatoma cell line, the Sec24A and Sec23B transcript levels were comparatively analysed in the stably HBV-expressing HepG2.2.15 and its parental HepG2 cell line. Again, the amount of Sec24A and Sec23B-specific mRNAs was clearly increased in HepG2.2.15 cells as compared with control cells (Figure 9a, b). Consistent with this, HBV replication augmented Sec24A protein levels (Figure 9c). In the case of Sec23B, we failed to verify its upregulation at the protein level, because commercially available antibodies malfunctioned (data not shown).

4 | DISCUSSION

HBV is currently estimated to have infected more than 250 million humans. The extremely successful spread of this pathogen among the human population is explained—among other factors—by its multiple particulate forms. Upon infection, HBV produce not only enveloped

FIGURE 8 Hepatitis B virus–coat protein complex II (HBV–COPII) interaction involves the N-terminal half of Sec24A and a di-arginine motif of HBV S. (a) HuH-7 cells were cotransfected with pNI2.S.HA and expression constructs encoding Myc-tagged versions of the long (Myc.Sec24A.l) or short (Myc.Sec24A.s) isoforms of Sec24A. Three days post transfection, cells were fixed with paraformaldehyde (PFA), permeabilized, and stained with S- (K38, green) and Myc-specific (red) antibodies. DNA staining is shown in blue. Overlain staining patterns (yellow) are displayed in the Merge panels with outlined areas showing enlargements. Bar, 10 μm. For quantitative colocalization analysis (QCA), Pearson correlation coefficient (PCC) values were calculated and represent the mean ± *SD* (left). Lysates of cotransfected cells were subjected to a Myc-specific Western blotting (WB). Numbers to the left refer to molecular weight markers in kDa (right). (b) Model of the transmembrane topology of S. The predicted four TM segments of the S protein project its N- and C-terminus into the endoplasmic reticulum (ER) lumen (equivalent to the outside of subviral envelope particle [SVPs]), thereby generating two cytosolic and one luminal loop. Numbers refer to aa positions, and the arginine residues (R78 and R79) terminating the first cytosolic loop are highlighted in red. N-Glycans partly linked to the luminal loop are denoted (G). (c) HuH-7 cells were transfected with Myc.Sec24A.s together with control plasmids (Con) or hemagglutinin (HA)-tagged versions of the wild-type or mutant S genes. Cell lysates were harvested after 3 days and assayed by Myc- and HA-specific WB to monitor protein expression (Input). For immunoprecipitation (IP), lysates were incubated with anti-S antibodies (K38) followed by Myc-specific WB. IgG.HC denotes IgG heavy chains. CO-IP analyses were done in triplicate, and a representative blot is shown. (d) Expression and secretion profile of wild-type and mutant S proteins. HuH-7 cells were transfected with the indicated constructs in duplicates for 3 days. Cell lysates (Cell) and concentrated cell supernatants (Medium) were examined with HA-specific WB. The p/gp forms of S are depicted. (e) HuH-7 cells were cotransfected with FLAG.Sec24A.s together with control plasmids (Con) or the indicated wild-type or mutant L_OHA genes. Protein synthesis was analysed by FLAG- and L-specific (K1350) WB of cell lysates (Input). The nonglycosylated (p39) and glycosylated (gp42) forms of L are indicated. Lysates were reacted with anti-S domain antibodies (K38; IP) and subjected to FLAG-specific WB. A representative blot of three independent experiments is shown

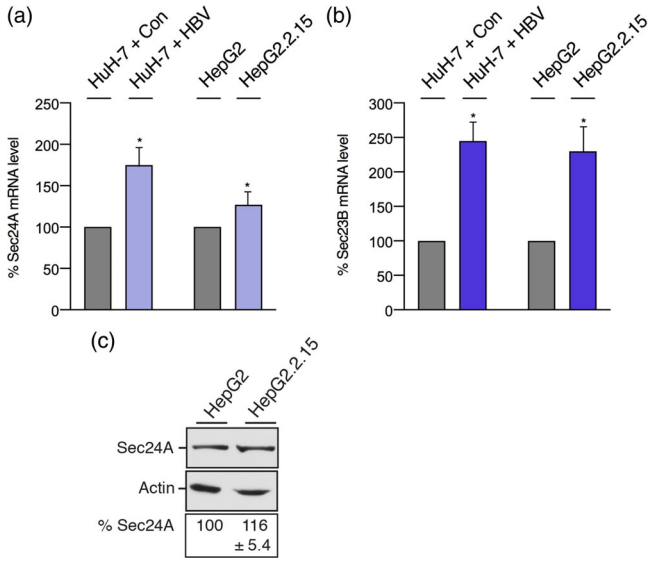

FIGURE 9 Hepatitis B virus (HBV) upregulates Sec24A and Sec23B transcript levels. (a) For transient HBV expression, HuH-7 cells were mock-transfected (HuH-7 + Con) or transfected with the pHBV replicon for 72 h (HuH-7 + HBV). For stable HBV expression, the HepG2.2.15 cell line was cultivated. Its parental HepG2 cell served as a negative control. Total mRNAs were isolated, reverse transcribed, and used for Sec24A-specific quantitative reverse transcription PCR (qRT-PCR) reactions. Fold changes in Sec24A gene expression were calculated by comparing mRNA levels in control- or HBV-expressing cells using β-actin as an endogenous reference gene. Error bars indicate the standard deviations from the mean of two experiments measured in duplicates. (b) Total mRNAs were isolated from cells and subjected to Sec23B-specific qRT-PCR reactions, exactly as outlined above. (c) Equal cell numbers of HepG2 and HepG2.2.15 cells were lysed and subjected to Sec24A- and β-actin-specific Western blotting (WB). Sec24A protein levels were quantitated and demonstrated in percent amount relative to control cells (n = 3, ±*SD*), and a representative blot is shown

progeny virions but also subviral empty envelope particles (SVPs) that together contribute to viral persistence and pathogenesis. In this report, we examined HBV SVP trafficking through the cell secretory pathway and found that the pathogen usurps distinct components of the COPII vesicle forming machinery for SVP host cell exit.

One important outcome of this work was the finding that the HBV S envelope protein is a specific Sec24A-dependent COPII cargo. The four mammalian Sec24 paralogs can be divided into two subclasses, Sec24A/B and Sec24C/D, sharing about 60% sequence identity within but only 25% identity across subclasses (Pagano et al., 1999). Expression profiling had shown that all four Sec24 paralogs are expressed in the liver of mice and humans (Adams, Chen, O'Shea, & Ginsburg, 2014; Chen et al., 2013; Pagano et al., 1999) and likewise in the HuH-7 liver cell line, as evidenced by transcript level analysis (see Figure S2a). Hence, our finding that the loss of Sec24A disrupted HBV S envelope ER exiting and cellular secretion without compensation by the three other Sec24 isoforms, in particular by the closely Sec24B paralog, was entirely unexpected. This is in contrast to previous studies demonstrating that the members of the two Sec24 subfamilies serve partially overlapping functions. Data from a genome-wide RNAi screening showed that depletion of individual Sec24 isoforms does not inhibit the transport of the vesicular stomatitis virus glycoprotein G (VSV-G). Rather, the combined loss of Sec24A and Sec24B is required to block VSV-G trafficking (Simpson et al., 2012). Similarly, the anterograde trafficking of the *Shaker* voltage-gated potassium channel subfamily member 3 (Kv1.3) could only be blocked by a double KD of Sec24A and Sec24B (Spear et al., 2015). In mice, a genetic deficiency of Sec24A is compatible with normal survival and development, although these animals display low plasma cholesterol levels as a result of impaired secretion of PCSK9, a regulator of blood cholesterol levels (Chen et al., 2013). COPII-dependent secretion of PCSK9 was shown to be selectively mediated by Sec24A and to a smaller extent by Sec24B, suggesting a partial overlap in functions of these two isoforms.

To account for the intrinsic selectivity of the HBV S envelope protein for Sec24A, we suspect specific protein–protein interactions. Our Y2H data demonstrated a direct physical interaction between the HBV S domain and Sec24A, reminiscent of typical cargo/COPII adaptor interactions. Intriguingly, mapping analysis revealed that the short form of Sec24A, derived from alternative splicing, is sufficient to interact with S. Hence, recognition sites for S must reside within the N-terminal half of Sec24A (i.e., aa 1–613). Sec24A and Sec24B share highly conserved C-terminal domains but differ in their hypervariable N-terminal segments comprising only 20% sequence identity (Pagano et al., 1999). We thus infer that the dispensability of Sec24B in HBV SVP export may rely on its inability to recognize S.

Structural and functional studies have revealed distinct cargo binding sites among Sec24 paralogs that recognize different sorting signals on diverse proteins, encompassing simple linear motifs and folded epitopes. In favour with this, we herein identified two consecutive arginine residues (R78 and R79), terminating the cytosolically exposed loop of S, that are essential for the interaction with Sec24A. The diminished affinity of the S mutants to Sec24A coincided with their defects in secretion, implicating that the dibasic R78/79 motif resembles a bona fide ER export code. Remarkably, this motif, which is conserved in all eight HBV genotypes, likewise mediates the interaction between Sec24A and the HBV L envelope protein. A related motif, comprising three arginine residues (3R), had been recently mapped within a cytosolic loop of the transmembrane α_{2B}-adrenergic receptor (Dong et al., 2012). Mutational analyses revealed that the 3R motif controls α_{2B}-adrenergic receptor exit from the ER and cell surface transport. However, unlike the R78/79 motif of the HBV envelope, the 3R export signal preferentially interacts with the Sec24C and Sec24D paralogs (Dong et al., 2012).

Moreover, we identified Sec23B to be crucial for HBV S envelope ER export. Curiously, we again discovered an isoform selectivity, as the virus specifically engaged Sec23B, but not Sec23A, for intracellular trafficking. The two human isoforms of Sec23, Sec23A and Sec23B, are ~85% identical to one another and largely redundant in function. As evidenced by interactome analyses, both isoforms interact with any of the four Sec24 isoforms without any differences in paralog specificity (Khoriaty et al., 2018; Khoriaty et al., 2017). Their

functional equivalence is supported by the findings that both human Sec23 paralogs are able to complement the function of yeast Sec23p and that the *Sec23a*-coding sequence inserted into the endogenous murine *Sec23b* locus fully rescues the mortality of Sec23B-deficient mice (Khoriaty et al., 2018). In line with this, the specific Sec23B perturbation phenotype, observed herein for HBV, was surprising.

However, a recent study demonstrated that the Sec23 paralogs can differ in functions due to posttranslational modifications (Jeong et al., 2018). There is growing evidence that COPII vesicles also promote autophagosome biogenesis by providing membranes, a process critically guided by Sec23B (Jeong et al., 2018). Under non-autophagic conditions, Sec23B, but not Sec23A, is targeted by the F-box protein FBXW5 for proteasomal degradation. Upon induction of autophagy, the Unc-51-like kinase is activated, which phosphorylates Sec23B, thereby preventing the interaction of Sec23B with FBXW5 and, thus, inhibiting Sec23B destruction. Stabilized Sec23B then associates with Sec24, thereby supporting COPII-mediated autophagosome formation (Jeong et al., 2018). HBV and even the sole expression of its S protein had been shown to induce autophagy (Doring, Zeyen, Bartusch, & Prange, 2018; J. Li et al., 2011; Sir et al., 2010). Accordingly, it is tempting to speculate that the HBV-induced autophagy may likewise increase Sec23B levels to benefit SVP egress. In line with this, we found an upregulation of Sec23B and also Sec24A transcript/protein levels in HBV-replicating HuH-7 and HepG2.2.15 cell lines. Although the precise underlying mechanisms remain to be defined, the expression changes of these two COPII components may meet the needs of HBV to drive effective SVP trafficking and export.

The HBV S protein is an unusual viral protein, as it is initially synthesized in a transmembrane configuration and then buds into the lumen of secretory organelles as soluble lipoprotein particles. The direct physical S-Sec24A interaction together with the involvement of the cytosolically disposed R78/79 motif strongly suggests that Sec24A recognizes and captures transmembrane S chains for COPII-guided transport to the ERGIC. Accordingly, intraluminal SVP budding should occur beyond the ER. This interpretation fits to a previous model deduced from biochemical studies that predicted that transmembrane S monomers rapidly form disulfide-linked dimers, catalysed by the ER chaperone protein disulfide-isomerase (PDI). Transmembrane dimers are next transported to the ERGIC where the absence of PDI and a different environment allow intraluminal SVP budding (Huovila et al., 1992). According to another model, transmembrane S dimers are predicted to form filamentous, rod-like structures within the ER that are transferred by ER-derived vesicles to the ERGIC where they are unpacked and relaxed before being converted into spherical particles for secretion (Patient et al., 2009). Because a direct S-Sec24A interaction appears implausible, if S would already have budded into the ER lumen, the filamentous structures, observed in situ by Patient et al. (2009), likely encompass transmembrane S molecules. As a prerequisite of S budding, approximately 48 S dimers must oligomerize conjoint with a selective exclusion of host proteins (Huovila et al., 1992; Patient et al., 2009; Prange, 2012). As exemplified for the VSV-G protein, its di-acidic ER export signal not only mediates capture by Sec24 but also directs its concentration into the budding COPII vesicles (Nishimura & Balch, 1997; Nishimura et al., 1999). Similarly, the recognition of S by Sec24A may aid to increase the local concentration of S required for its proper self-assembly.

In case of no ER exit, provoked by COPII silencing or BFA treatment, the intracellular staining pattern of S changed, as it now appeared in dot-like structures. Thus far, these structures are unknown but may resemble S aggregates or misfolded polymers. Similar observations had been made, for example, naturally occurring mutants of α1-anti-trypsin that are blocked in ER export and secretion and accumulated in form of polymers in the ER (Anelli & Panina-Bordignon, 2019).

The presently available antiviral treatments for HBV infection reduce viral replication but do not affect SVP levels in the blood (Revill et al., 2019). In infected patients, SVPs constitute the bulk of circulating viral particles and are thought to exhaust B and T cell responses, to interfere with signaling in adaptive and innate immune function, and to contribute to viral persistence (Hu & Liu, 2017; Mohebbi et al., 2018). New approaches to treating HBV include an interference with SVP trafficking and secretion (Mohebbi et al., 2018). Candidate compounds include nucleic acid polymers (NAPs), cell-permeable phosphorothioate oligonucleotides that had been shown to selectively inhibit SVP assembly/release in vitro and in vivo (Blanchet, Sinnathamby, Vaillant, & Labonte, 2019). Because NAPs can clear SVPs from the blood without any discernible direct interaction with HBV components, they are thought to target host proteins selectively involved in viral envelope trafficking (Beilstein, Blanchet, Vaillant, & Sureau, 2018). Given the pronounced selectivity of the HBV envelope for certain COPII components, it is tempting to hypothesize that NAPs may attack Sec24A and/or Sec23B. In any case, a perturbation of the HBV–COPII interaction may be a means for host-targeted antiviral interventions.

This study is the first to document an essential role of the COPII machinery in HBV's pathogenic life cycle. HBV is yet another example of COPII cargo adaptor takeover by viral pathogens, encompassing VSV (Nishimura & Balch, 1997), the turnip mosaic virus (Jiang, Patarroyo, Garcia Cabanillas, Zheng, & Laliberte, 2015), HCV (Syed et al., 2017), and the Ebola virus (Yamayoshi et al., 2008). Together, those reports and our study add clues for pathogen-specific exploitation of special COPII coats for host cell exit with potential implications for cell biology, virology, and antiviral drug designs.

ACKNOWLEDGMENT

We thank Karin Awe and Camille Sureau for generously providing plasmid DNA constructs and for the experimental support. This work was supported by grants to R. P. from the Deutsche Forschungsgemeinschaft (PR 305/3-2/3-3).

CONFLICT OF INTEREST

The authors have no competing financial interests and are solely responsible for the experimental designs and data analysis.

AUTHOR CONTRIBUTIONS

L. Z., T. D., and R. P. conceived and designed the experiments. L. Z. and T. D. performed the experiments. L. Z., J. S., and R. P. analysed

the data. R. P. oversaw the project and wrote the manuscript. All authors discussed and edited the manuscript.

ORCID

Lisa Zeyen https://orcid.org/0000-0002-9594-6485
Reinhild Prange https://orcid.org/0000-0001-8312-4970

REFERENCES

Adams, E. J., Chen, X. W., O'Shea, K. S., & Ginsburg, D. (2014). Mammalian COPII coat component SEC24C is required for embryonic development in mice. *The Journal of Biological Chemistry*, *289*(30), 20858–20870. https://doi.org/10.1074/jbc.M114.566687

Anelli, T., & Panina-Bordignon, P. (2019). How to avoid a no-deal ER exit. *Cells*, *8*(9). https://doi.org/10.3390/cells8091051

Awe, K. (2009). PhD Thesis, The University of Mainz. 2009. Characterization of cellular interaction partners of the large envelope protein of the hepatitis B virus. Available from: https://publications.ub.uni-mainz.de/theses/volltexte/2009/2108/pdf/2108.pdf.

Barlowe, C., & Helenius, A. (2016). Cargo capture and bulk flow in the early secretory pathway. *Annual Review of Cell and Developmental Biology*, *32*, 197–222. https://doi.org/10.1146/annurev-cellbio-111315-125016

Beilstein, F., Blanchet, M., Vaillant, A., & Sureau, C. (2018). Nucleic acid polymers are active against hepatitis delta virus infection in vitro. *Journal of Virology*, *92*(4), JVI.01416–JVI.01417. https://doi.org/10.1128/jvi.01416-17

Bethune, J., & Wieland, F. T. (2018). Assembly of COPI and COPII vesicular coat proteins on membranes. *Annual Review of Biophysics*, *47*, 63–83. https://doi.org/10.1146/annurev-biophys-070317-033259

Blanchet, M., Sinnathamby, V., Vaillant, A., & Labonte, P. (2019). Inhibition of HBsAg secretion by nucleic acid polymers in HepG2.2.15 cells. *Antiviral Research*, *164*, 97–105. https://doi.org/10.1016/j.antiviral.2019.02.009

Blondot, M. L., Bruss, V., & Kann, M. (2016). Intracellular transport and egress of hepatitis B virus. *Journal of Hepatology*, *64*(1 Suppl), S49–S59. https://doi.org/10.1016/j.jhep.2016.02.008

Bruss, V. (1997). A short linear sequence in the pre-S domain of the large hepatitis B virus envelope protein required for virion formation. *Journal of Virology*, *71*(12), 9350–9357.

Chen, X. W., Wang, H., Bajaj, K., Zhang, P., Meng, Z. X., Ma, D., … Ginsburg, D. (2013). SEC24A deficiency lowers plasma cholesterol through reduced PCSK9 secretion. *eLife*, *2*, e00444. https://doi.org/10.7554/eLife.00444

Chou, S. F., Tsai, M. L., Huang, J. Y., Chang, Y. S., & Shih, C. (2015). The dual role of an ESCRT-0 component HGS in HBV transcription and naked capsid secretion. *PLoS Pathogens*, *11*(10), e1005123. https://doi.org/10.1371/journal.ppat.1005123

Dong, C., Nichols, C. D., Guo, J., Huang, W., Lambert, N. A., & Wu, G. (2012). A triple arg motif mediates alpha(2B)-adrenergic receptor interaction with Sec24C/D and export. *Traffic*, *13*(6), 857–868. https://doi.org/10.1111/j.1600-0854.2012.01351.x

Doring, T., Zeyen, L., Bartusch, C., & Prange, R. (2018). Hepatitis B virus subverts the autophagy elongation complex Atg5-12/16L1 and does not require Atg8/LC3 lipidation for viral maturation. *Journal of Virology*, *92*(7). https://doi.org/10.1128/jvi.01513-17

Hartmann-Stuhler, C., & Prange, R. (2001). Hepatitis B virus large envelope protein interacts with gamma2-adaptin, a clathrin adaptor-related protein. *Journal of Virology*, *75*(11), 5343–5351. https://doi.org/10.1128/JVI.75.11.5343-5351.2001

Hu, J., & Liu, K. (2017). Complete and incomplete hepatitis B virus particles: Formation, function, and application. *Viruses*, *9*(3). https://doi.org/10.3390/v9030056

Hu, J., & Seeger, C. (2015). Hepadnavirus genome replication and persistence. *Cold Spring Harbor Perspectives in Medicine*, *5*(7), a021386. https://doi.org/10.1101/cshperspect.a021386

Huovila, A. P., Eder, A. M., & Fuller, S. D. (1992). Hepatitis B surface antigen assembles in a post-ER, pre-Golgi compartment. *The Journal of Cell Biology*, *118*(6), 1305–1320. https://doi.org/10.1083/jcb.118.6.1305

Jeong, Y. T., Simoneschi, D., Keegan, S., Melville, D., Adler, N. S., Saraf, A., … Pagano, M. (2018). The ULK1-FBXW5-SEC23B nexus controls autophagy. *eLife*, *7*. https://doi.org/10.7554/eLife.42253

Jiang, B., Himmelsbach, K., Ren, H., Boller, K., & Hildt, E. (2015). Subviral hepatitis B virus filaments, like infectious viral particles, are released via multivesicular bodies. *Journal of Virology*, *90*(7), 3330–3341. https://doi.org/10.1128/jvi.03109-15

Jiang, J., Patarroyo, C., Garcia Cabanillas, D., Zheng, H., & Laliberte, J. F. (2015). The vesicle-forming 6K2 protein of turnip mosaic virus interacts with the COPII coatomer Sec24a for viral systemic infection. *Journal of Virology*, *89*(13), 6695–6710. https://doi.org/10.1128/jvi.00503-15

Khoriaty, R., Hesketh, G. G., Bernard, A., Weyand, A. C., Mellacheruvu, D., Zhu, G., … Ginsburg, D. (2018). Functions of the COPII gene paralogs SEC23A and SEC23B are interchangeable in vivo. *Proceedings of the National Academy of Sciences of the United States of America*, *115*(33), E7748-e7757. https://doi.org/10.1073/pnas.1805784115

Khoriaty, R., Vogel, N., Hoenerhoff, M. J., Sans, M. D., Zhu, G., Everett, L., … Williams, J. A. (2017). SEC23B is required for pancreatic acinar cell function in adult mice. *Molecular Biology of the Cell*, *28*(15), 2146–2154. https://doi.org/10.1091/mbc.E17-01-0001

Kirchhausen, T. (2000). Three ways to make a vesicle. *Nature Reviews. Molecular Cell Biology*, *1*(3), 187–198. https://doi.org/10.1038/35043117

Lambert, C., Mann, S., & Prange, R. (2004). Assessment of determinants affecting the dual topology of hepadnaviral large envelope proteins. *The Journal of General Virology*, *85*(Pt 5), 1221–1225. https://doi.org/10.1099/vir.0.19737-0

Lambert, C., Thome, N., Kluck, C. J., & Prange, R. (2004). Functional incorporation of green fluorescent protein into hepatitis B virus envelope particles. *Virology*, *330*(1), 158–167. https://doi.org/10.1016/j.virol.2004.09.031

Li, J., Liu, Y., Wang, Z., Liu, K., Wang, Y., Liu, J., … Yuan, Z. (2011). Subversion of cellular autophagy machinery by hepatitis B virus for viral envelopment. *Journal of Virology*, *85*(13), 6319–6333. https://doi.org/10.1128/jvi.02627-10

Li, W. (2015). The hepatitis B virus receptor. *Annual Review of Cell and Developmental Biology*, *31*, 125–147. https://doi.org/10.1146/annurev-cellbio-100814-125241

Loffler-Mary, H., Dumortier, J., Klentsch-Zimmer, C., & Prange, R. (2000). Hepatitis B virus assembly is sensitive to changes in the cytosolic S loop of the envelope proteins. *Virology*, *270*(2), 358–367. https://doi.org/10.1006/viro.2000.0268

McCaughey, J., & Stephens, D. J. (2018). COPII-dependent ER export in animal cells: Adaptation and control for diverse cargo. *Histochemistry and Cell Biology*, *150*(2), 119–131. https://doi.org/10.1007/s00418-018-1689-2

Miller, E. A., & Schekman, R. (2013). COPII—A flexible vesicle formation system. *Current Opinion in Cell Biology*, *25*(4), 420–427. https://doi.org/10.1016/j.ceb.2013.04.005

Mohebbi, A., Lorestani, N., Tahamtan, A., Kargar, N. L., & Tabarraei, A. (2018). An overview of hepatitis B virus surface antigen secretion inhibitors. *Frontiers in Microbiology*, *9*, 662. https://doi.org/10.3389/fmicb.2018.00662

Nassal, M. (2008). Hepatitis B viruses: Reverse transcription a different way. *Virus Research*, *134*(1–2), 235–249. https://doi.org/10.1016/j.virusres.2007.12.024

Nebenfuhr, A., Ritzenthaler, C., & Robinson, D. G. (2002). Brefeldin A: Deciphering an enigmatic inhibitor of secretion. *Plant Physiology*, *130*(3), 1102–1108. https://doi.org/10.1104/pp.011569

Nishimura, N., & Balch, W. E. (1997). A di-acidic signal required for selective export from the endoplasmic reticulum. *Science*, *277*(5325), 556–558. https://doi.org/10.1126/science.277.5325.556

Nishimura, N., Bannykh, S., Slabough, S., Matteson, J., Altschuler, Y., Hahn, K., & Balch, W. E. (1999). A di-acidic (DXE) code directs concentration of cargo during export from the endoplasmic reticulum. *The Journal of Biological Chemistry*, *274*(22), 15937–15946. https://doi.org/10.1074/jbc.274.22.15937

Pagano, A., Letourneur, F., Garcia-Estefania, D., Carpentier, J. L., Orci, L., & Paccaud, J. P. (1999). Sec24 proteins and sorting at the endoplasmic reticulum. *The Journal of Biological Chemistry*, *274*(12), 7833–7840. https://doi.org/10.1074/jbc.274.12.7833

Patient, R., Hourioux, C., & Roingeard, P. (2009). Morphogenesis of hepatitis B virus and its subviral envelope particles. *Cellular Microbiology*, *11*(11), 1561–1570. https://doi.org/10.1111/j.1462-5822.2009.01363.x

Prange, R. (2012). Host factors involved in hepatitis B virus maturation, assembly, and egress. *Medical Microbiology and Immunology*, *201*(4), 449–461. https://doi.org/10.1007/s00430-012-0267-9

Revill, P. A., Chisari, F. V., Block, J. M., Dandri, M., Gehring, A. J., Guo, H., … Zoulim, F. (2019). A global scientific strategy to cure hepatitis B. *The Lancet Gastroenterology & Hepatology*, *4*(7), 545–558. https://doi.org/10.1016/s2468-1253(19)30119-0

Rost, M., Mann, S., Lambert, C., Doring, T., Thome, N., & Prange, R. (2006). Gamma-adaptin, a novel ubiquitin-interacting adaptor, and Nedd4 ubiquitin ligase control hepatitis B virus maturation. *The Journal of Biological Chemistry*, *281*(39), 29297–29308. https://doi.org/10.1074/jbc.M603517200

Rout, M. P., & Field, M. C. (2017). The evolution of organellar coat complexes and organization of the eukaryotic cell. *Annual Review of Biochemistry*, *86*, 637–657. https://doi.org/10.1146/annurev-biochem-061516-044643

Simpson, J. C., Joggerst, B., Laketa, V., Verissimo, F., Cetin, C., Erfle, H., … Pepperkok, R. (2012). Genome-wide RNAi screening identifies human proteins with a regulatory function in the early secretory pathway. *Nature Cell Biology*, *14*(7), 764–774. https://doi.org/10.1038/ncb2510

Sir, D., Tian, Y., Chen, W. L., Ann, D. K., Yen, T. S., & Ou, J. H. (2010). The early autophagic pathway is activated by hepatitis B virus and required for viral DNA replication. *Proceedings of the National Academy of Sciences of the United States of America*, *107*(9), 4383–4388. https://doi.org/10.1073/pnas.0911373107

Spear, J. M., Koborssy, D. A., Schwartz, A. B., Johnson, A. J., Audhya, A., Fadool, D. A., & Stagg, S. M. (2015). Kv1.3 contains an alternative C-terminal ER exit motif and is recruited into COPII vesicles by Sec24a. *BMC Biochemistry*, *16*, 16. https://doi.org/10.1186/s12858-015-0045-6

Stieler, J. T., & Prange, R. (2014). Involvement of ESCRT-II in hepatitis B virus morphogenesis. *PLoS One*, *9*(3), e91279. https://doi.org/10.1371/journal.pone.0091279

Stirk, H. J., Thornton, J. M., & Howard, C. R. (1992). A topological model for hepatitis B surface antigen. *Intervirology*, *33*(3), 148–158. https://doi.org/10.1159/000150244

Suffner, S., Gerstenberg, N., Patra, M., Ruibal, P., Orabi, A., Schindler, M., & Bruss, V. (2018). Domains of the hepatitis B virus small surface protein S mediating oligomerization. *Journal of Virology*, *92*(11). https://doi.org/10.1128/jvi.02232-17

Syed, G. H., Khan, M., Yang, S., & Siddiqui, A. (2017). Hepatitis C virus lipoviroparticles assemble in the endoplasmic reticulum (ER) and bud off from the ER to the Golgi compartment in COPII vesicles. *Journal of Virology*, *91*(15). https://doi.org/10.1128/jvi.00499-17

Wang, Z., Yu, G., Liu, Y., Liu, S., Aridor, M., Huang, Y., … Wang, Q. K. (2018). Small GTPases SAR1A and SAR1B regulate the trafficking of the cardiac sodium channel Nav1.5. *Biochimica et Biophysica Acta - Molecular Basis of Disease*, *1864*(11), 3672–3684. https://doi.org/10.1016/j.bbadis.2018.09.003

Watanabe, T., Sorensen, E. M., Naito, A., Schott, M., Kim, S., & Ahlquist, P. (2007). Involvement of host cellular multivesicular body functions in hepatitis B virus budding. *Proceedings of the National Academy of Sciences of the United States of America*, *104*(24), 10205–10210. https://doi.org/10.1073/pnas.0704000104

Wendeler, M. W., Paccaud, J. P., & Hauri, H. P. (2007). Role of Sec24 isoforms in selective export of membrane proteins from the endoplasmic reticulum. *EMBO Reports*, *8*(3), 258–264. https://doi.org/10.1038/sj.embor.7400893

Yamayoshi, S., Noda, T., Ebihara, H., Goto, H., Morikawa, Y., Lukashevich, I. S., … Kawaoka, Y. (2008). Ebola virus matrix protein VP40 uses the COPII transport system for its intracellular transport. *Cell Host & Microbe*, *3*(3), 168–177. https://doi.org/10.1016/j.chom.2008.02.001

SUPPORTING INFORMATION

Additional supporting information may be found online in the Supporting Information section at the end of this article.

How to cite this article: Zeyen L, Döring T, Stieler JT, Prange R. Hepatitis B subviral envelope particles use the COPII machinery for intracellular transport via selective exploitation of Sec24A and Sec23B. *Cellular Microbiology*. 2020;22:e13181. https://doi.org/10.1111/cmi.13181